Electronic Supplementary Material (ESI) for Journal of Materials Chemistry C.

Energy-storage performance of $NaNbO_3$ based multilayer capacitors

Li-Feng Zhu[1,2,3], Yongke Yan*[2], Haoyang Leng[2], Xiaotian Li[2], Li-Qian Cheng[2], Shashank Priya*[2]

[1] School of Materials Science and Engineering, University of Science and Technology Beijing, Beijing 100083, China.

[2] Department of Materials Science and Engineering, The Pennsylvania State University, University Park, PA 16802, United States

[3] Foshan (Southern China) Institute for New Materials, Foshan, Guangdong, 528200, China.

Figure S1 shows the XRD spectra of the NN-0.4CZ-*x*BNT ceramics at $0.12 \leq x \leq 0.18$. All samples exhibit pure perovskite structure without noticeable any impurity phase within the detectable limit of the XRD, suggesting the formation of a stable solid solution. The standard diffraction peaks cited from $NaNbO_3$ with the orthorhombic phase (*O*-phase, PDF#33-1270, Pbma, antiferroelectric phase) and cubic phase (*C*-phase PDF#75-2102, Pm-3m, paraelectric phase) are indicated by vertical lines for comparison. The diffraction peaks of the samples at $0.12 \leq x \leq 0.18$ correspond well to *C* phase. However, different the PDF#75-2102 of *C* phase, there are two peaks around 46.5° and 58°, respectively, in the samples at $0.12 \leq x \leq 0.18$ as

Corresponding author: yxy355@psu.edu (Yongke Yan)
Corresponding author: sup103@psu.edu (Shashank Priya)

shown in Fig.S1b. This shows that the phase structure of samples at $0.12 \leq x \leq 0.18$ is not a single *C* phase, but consists of *C* and *O* two phases, In addition, the characteristic peaks around 36.5° of the antiferroelectric *O* phase are also found in all samples as shown in Fig.S2, which further proves that the antiferroelectric *O* phase exists in the samples of $0.12 \leq x \leq 0.18$.

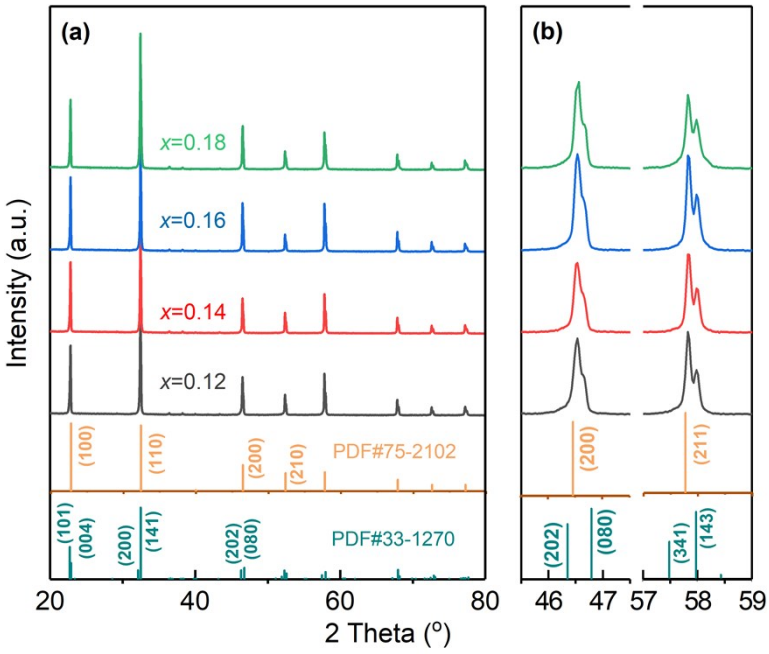

Figure S1 X-ray di□raction patterns of the NN-0.04CZ-*x*BNT ceramics with different *x* content ($0.12 \leq x \leq 0.18$) in a selected 2θ range of 20°-80° (a), 45.5°-47.5° and 57°-59° (b)

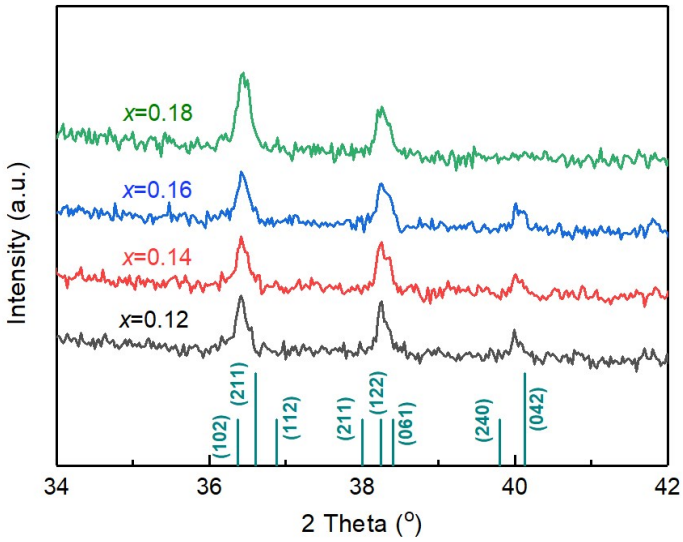

Figure S2 X-ray di□raction patterns of the NN-0.04CZ-*x*BNT ceramics with different *x* content ($0.12 \leq x \leq 0.18$) in a selected 2θ range of 34°-42°

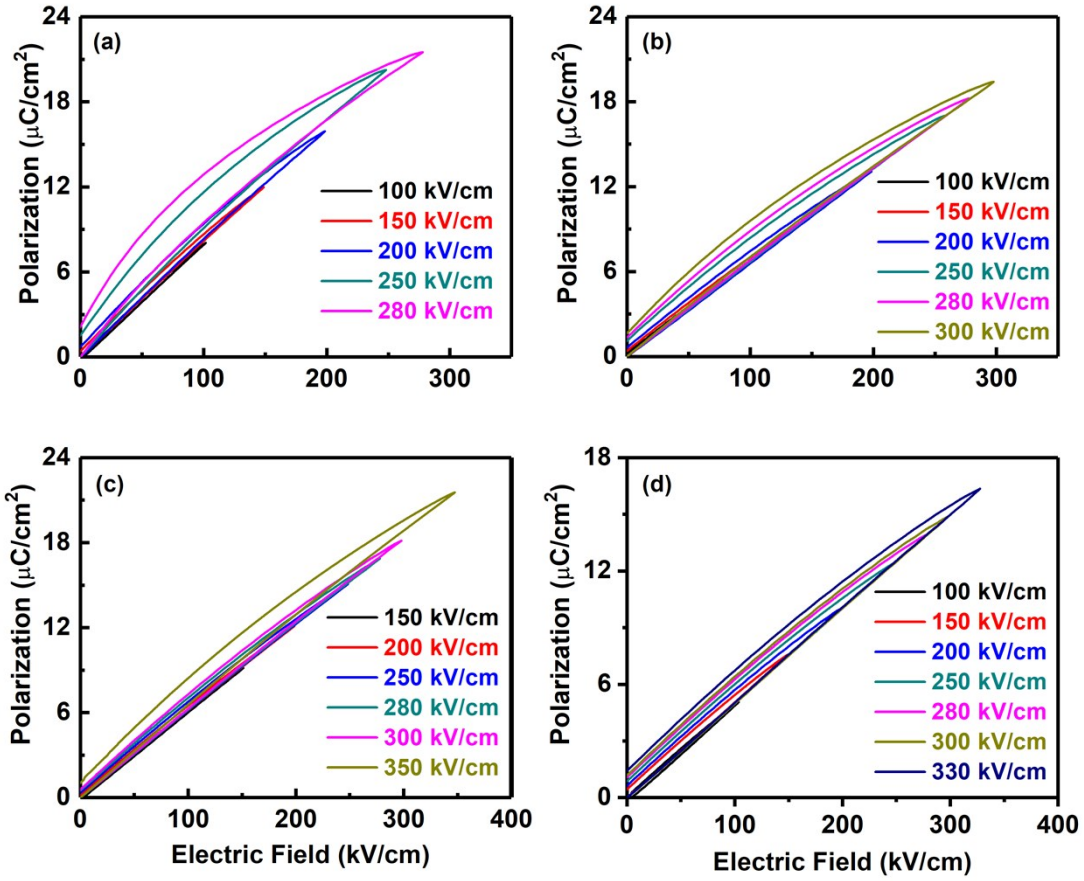

Figure S3 Unipolar P-E loops of NN-0.04CZ-*x*BNT ceramics with different *x* content, *x*=0.12 (a), *x*=0.14 (b), *x*=0.16 (c), and *x*=0.18 (d)

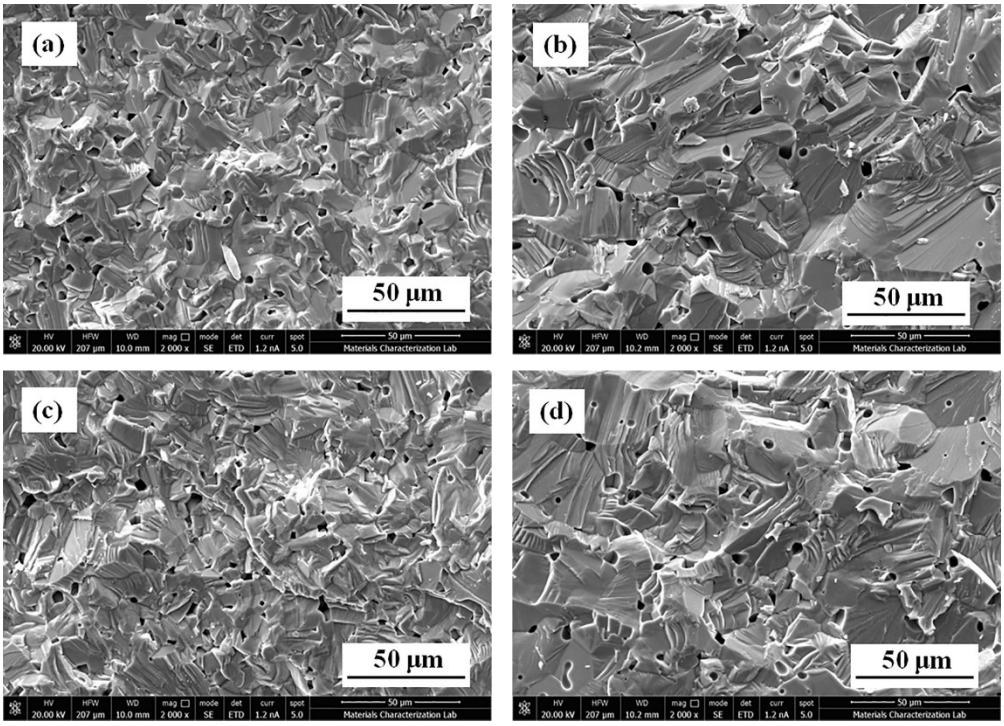

Figure S4 SEM images of fracture surface for 0.80NN-0.04CZ-0.16BNT ceramics with different x content, x=0.12 (a), x=0.14 (b), x=0.16 (c), and x=0.18 (d)

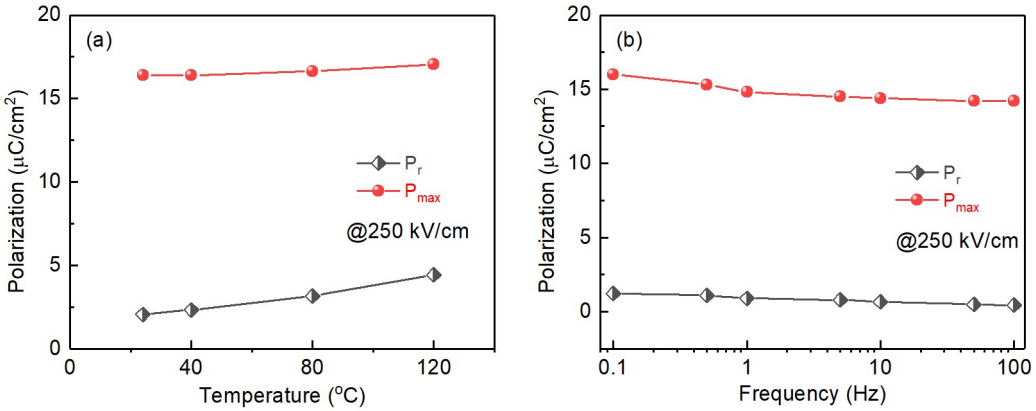

Figure S5 Variation of P_{max} and P_r versus the temperature (a) and frequency (b) for 0.80NN-0.04CZ-0.16BNT ceramics